Versatility of Aqueous Micellar Solutions for Self-Assembled Monolayers Engineering

Lionel Patrone,*,†,‡ Serge Palacin,§ Jean-Philippe Bourgoin,*,† and Martinus H. V. Werts†,||

CEA/DSM/DRECAM/Service de Chimie Moléculaire, Bât. 125, and CEA/DSM/DRECAM/Service de Physique et Chimie des Surfaces et des Interfaces, CEA/Saclay, F-91191 Gif-sur-Yvette Cedex, France

Received July 24, 2004. In Final Form: September 24, 2004

Self-assembly of aliphatic as well as aromatic thiol-terminated molecules was achieved onto a variety of gold surfaces using aqueous micellar solutions. Scanning tunneling microscopy experiments allowed us to demonstrate that the increase in the density of self-assembled monolayers (SAMs) prepared from micellar aqueous solvent compared to that prepared from ethanol directly originates from the decrease in defect density in the SAM (etch pits, domain boundaries) and not from a denser local packing of the molecules. Extending the use of such an aqueous solvent to various conjugated molecules, we report for the first time the insertion of these molecules from an aqueous solution in a dodecanethiol (DT) SAM and the ligand-exchange on the surface of DT stabilized gold nanoparticles deposited as a Langmuir−Blodgett film. Finally, we show that aqueous micellar DT solutions allow the preparation of DT SAMs on gold through a micropatterned resist mask. These results make possible the use of water to deliver molecules on a solid substrate to build molecular devices in a way compatible with lithography requirements in microelectronic processes.

Introduction

Self-assembly, defined following Whitesides and Grzybowski as a process that involves preexisting components, is reversible, can be controlled by proper design of the components, and is attractive for many reasons.[1] These include in particular the fact that self-assembly is one of the few practical strategies for making ensembles of nanostructures. It will, therefore, be an essential part of nanotechnology. Considering, for example, the rapidly developing field of molecular electronics, self-assembly is generally believed to be the future key enabling technology for fabrication of dense circuits involving billions of nanoobjects.[2] So far, though this particular field is still in its infancy, self-assembly processes and self-assembled monolayers (SAMs), in particular, are already used for fabricating research devices and circuits.[2−4] SAMs are used either for surface functionalization to provide passivation,[5] for control of work function and contact energetics,[6−8] for directed deposition,[9−11] or as the functional layer like in the scanning tunneling microscopy (STM), nanopore, mechanical break junction, or recently developed molecular transport measurement techniques (see refs 2−4 and 12).

Further developing the use of SAMs in molecular electronics requires addressing the following key issues: mastering the preparation of dense, defect-free, ordered SAMs of controlled composition over large areas, because the quality of the SAMs directly controls its impermeability (against electrical defects and short-circuit formation when evaporating a metallic electrode on top of the SAM) and rendering SAM formation processes compatible with lithographic techniques.

The solvent used for the SAM preparation directly impacts these two points. SAMs are usually prepared by immersion of the substrate in a solution of the molecules to be self-assembled.[13] These solutions are prepared using organic solvents (ethanol, isooctane, hexane, chloroform, ...) which are efficient for solvating both long aliphatic and conjugated molecules. This organic solvent-based process has a number of important drawbacks. These include the volatility, toxicity, and waste disposal problems of the solvent. Moreover, some of them do not lead to high-quality SAMs[14] or prevent the use of self-assembly techniques in micro-nanofabrication because they are incompatible with the use of resists. The former point is evidenced for example in the case of chloroform with

* To whom correspondence should be addressed. E-mail: lionel.patrone@l2mp.fr (L.P.); jbourgoin@cea.fr (J.-P.B.). Tel.: +33 4 94 03 89 50 (L.P.); +33 1 69 08 55 65 (J.-P.B.). Fax: +33 4 94 03 89 51 (L.P.); +33 1 69 08 66 40 (J.-P.B.).

† CEA/DSM/DRECAM/Service de Chimie Moléculaire, CEA/Saclay.

‡ Present address: CNRS-L2MP UMR 6137, ISEN-Toulon, Maison des Technologies, Place Georges Pompidou, 83000 Toulon, France.

§ CEA/DSM/DRECAM/Service de Physique et Chimie des Surfaces et des Interfaces, CEA/Saclay.

|| Present address: CNRS UMR 6510 (SESO), Université de Rennes 1, Campus de Beaulieu Bât. 10A, F-35042 Rennes Cedex, France.

(1) Whitesides, G. M.; Grzybowski, B. *Science* **2002**, *295*, 2418.
(2) Heath, J. R.; Ratner, M. A. *Phys. Today* **2003**, *56*, 43.
(3) Reed, M. A.; Tour, J. M. *Sci. Am.* **2000**, *282*, 86.
(4) Joachim, C.; Gimzewski, J. K.; Aviram, A. *Nature* **2000**, *408*, 546.
(5) Ashkenasy, G.; Cahen, D.; Cohen, R.; Shanzer, A.; Vilan, A. *Acc. Chem. Res.* **2002**, *35*, 121.
(6) Vuillaume, D. *J. Nanosci. Nanotechnol.* **2002**, *2*, 267.
(7) Cui, X. D.; Freitag, M.; Martel, R.; Brus, L.; Avouris, P. *Nano Lett.* **2003**, *3*, 783.
(8) Bumm, L. A.; Arnold, J. J.; Cygan, M. T.; Dunbar, T. D.; Burgin, T. P.; Jones, L.; Allara, D. L.; Tour, J. M.; Weiss, P. S. *Science* **1996**, *271*, 1705.
(9) Jie, L.; Casavant, M. J.; Cox, M.; Walters, D. A.; Boul, P.; Wei, L.; Rimberg, A. J.; Smith, K. A.; Colbert, D. T.; Smalley, R. E. *Chem. Phys. Lett.* **1999**, *303*, 125.
(10) Choi, K. H.; Bourgoin, J. P.; Auvray, S.; Esteve, D.; Duesberg, G. S.; Roth, S.; Burghard, M. *Surf. Sci.* **2000**, *462*, 195.
(11) Palacin, S.; Hidber, P. C.; Bourgoin, J. P.; Miramond, C.; Fermon, C.; Whitesides, G. M. *Chem. Mater.* **1996**, *8*, 1316.
(12) Hanggi, P.; Ratner, M.; Yaliraki, S. *Chem. Phys.* **2002**, *281*, 111.
(13) Ulman, A. *Chem. Rev.* **1996**, *96*, 1533.
(14) Yan, D.; Saunders, J. A.; Jennings, G. K. *Langmuir* **2003**, *19*, 9290.

10.1021/la048133b CCC: $27.50
Published on Web 11/20/2004

alkanethiolate molecules adsorbed onto gold. Indeed, after a few hours in the solvent, the quality of the SAM is altered, some molecules being removed from the assembly. These problems seriously prevent using SAMs prepared from organic solvents in future industrial nanotechnology processes.[15] Using water as a solvent instead offers a promising alternative. Previous work has shown that hydroxyl-terminated thiol SAMs could be formed on gold from an aqueous solution, forming compact and stable monolayers.[16] Using micelles to self-assemble dodecanethiol (DT) molecules, which are insoluble in water, constituted an important step forward. Liu and Kaifer prepared SAMs of DT on gold from aqueous micellar solutions of Triton X-100, sodium dodecyl sulfate, and hexadecyltrimethylammonium bromide above the critical micelle concentration (cmc).[17] These SAMs exhibited typical electrochemical properties (low capacitance, blocking of the voltammetric response), indicating that they were equivalent to the SAMs prepared from ethanolic solutions. More recently, Jennings et al. reported the preparation of *n*-alkanethiolate SAMs ($n = 8-18$) formed onto gold from an aqueous micellar solution,[14,18,19] in particular using nonpolar hexaethylene glycol monodecyl ether micelles ($C_{12}E_6$).[18] Interestingly, compared to the equivalent SAMs prepared from an ethanolic solution, these SAMs showed an overall increased chain density, as deduced from infrared spectroscopy experiments, and a higher electrochemical blocking ability.[18] These observations are in agreement with the work of Miller et al. who also reported more packed and more stable ω-hydroxy alkanethiols monolayers from aqueous solutions than those from ethanol.[16]

The issue of SAMs quality (cristallinity, low defect density) is crucial for their application in molecular electronics as well as in other domains. In this article, we focus on two types of SAMs prepared from an aqueous environment: DT SAMs, which are a prototype of insulating layers, and mixed SAMs of DT/conjugated molecules, which allow the conjugated molecules in a controlled environment to be addressed individually.[8,20-23] In the former case, we study specifically the quality of the SAMs prepared from $C_{12}E_6$ micelles by STM and by the kinetics of insertion of conjugated molecules into the layer. In the latter case, we demonstrate for the first time that using an aqueous micellar solvent for thiol-terminated conjugated molecules enables them to be inserted into SAMs of alkylthiol on gold surfaces, as well as to be place-exchanged with DT molecules of the surface of DT-stabilized gold nanoparticles. Finally, we show that preparing SAMs from aqueous micellar solution is compatible with standard electron-beam (e-beam) lithography.

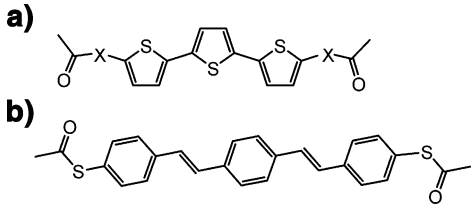

Figure 1. Schematic representation of the (a) X = S, 2,5″-bis(acetylthio)-5,2′5′,2″-terthienyl molecule (T3), or X = Se, 2,5″-bis(acetylseleno)-5,2′5′,2″-terthienyl molecule (Se3), and (b) OPV3 molecules, ~14- and ~20-Å long, respectively.

Experimental Section

Molecules. The conjugated molecules we used are shown in Figure 1. α,ω-Bis(acetylthio)terthiophene (T3) and α,ω-bis-(acetylseleno)terthiophene (Se3) were synthesized following the Miller's method. Bis(acetylthio)oligo(3-phenylene vinylene) (OPV3) has been prepared via McMurry and Wittig type reactions.[24] An acetyl group was used to protect the reactive thiol group and to increase the solubility. Such conjugated molecules are of great interest in the field of molecular electronics because of their electronic transport ability.[2,4]

Preparation of the Aqueous Micellar Solutions. Aqueous micellar solutions used in our experiments were prepared in two steps. First the aqueous solution of nonionic hexaethylene glycol monodecyl ether micelles ($C_{12}E_6$) was made with a concentration about 10 times higher than the desired thiol concentration in deionized water (18 MΩ·cm) following refs 18 (DT) and 25 (T3). We used a 10^{-3} M DT concentration and 5×10^{-4} M for the conjugated molecules, which means micelle concentrations of 10^{-2} M and 5×10^{-3} M, respectively. This ensures that we are working above the cmc of $C_{12}E_6$, which is between 7×10^{-5} and 10^{-4} M at 20 °C.[26] Then, we introduce the appropriate quantity of molecules in that solution. The same process as for T3 was used for Se3 and OPV3. DT molecules were easily solvated after a few minutes of sonication as in refs 17 and 18. As for the conjugated molecules (T3, Se3, OPV3), sonication was performed during several hours and followed by centrifugation (15 000 rpm during ~15 min). The clear supernatant was used after filtering through a 200-nm filter. UV−visible spectrophotometric measurements on the clear supernatant gave concentrations of 5×10^{-7} M for OPV3 and 2.5×10^{-6} M for T3 and Se3.

Sample Preparation. Gold surfaces, used as substrates for the STM experiments, were obtained by Joule evaporation of gold at a base pressure of a few 10^{-8} Torr onto freshly cleaved mica surfaces. During deposition, the mica substrates were heated at 340 °C and annealed up to 30 min after deposition. This provided good-quality epitaxial (111) Au surfaces with atomically flat terraces. For carrying out polarization modulation infrared reflection−absorption spectroscopy (PM-IRRAS) experiments, gold was evaporated on Cr-coated glass slides cleaned beforehand in freshly prepared Piranha solution (3:1 concentrated H_2SO_4/H_2O_2; CAUTION!).

Langmuir−Blodgett (LB) films of DT-stabilized gold nanoparticles were deposited on 30×10 mm^2 glass slides.[27] Prior to deposition, the glass slides were cleaned in Piranha solution. After extensive rinsing and drying under a nitrogen flow, the slides were silanized overnight by storing them in a sealed container with a few droplets of 1,1,1,3,3,3-hexamethyldisilazane. This gas-phase procedure yields glass substrates of low surface

(15) SAMs formed by microcontact printing [(a) Xia, Y.; Whitesides, G. M. *Langmuir* **1997**, *13*, 2059. (b) Xia, Y.; Whitesides, G. M. *Angew. Chem., Int. Ed.* **1998**, *37*, 551. (c) Michel, B.; Bernard, A.; Bietsch, A.; Delamarche, E.; Geissler, M.; Juncker, D.; Kind, H.; Renault, J. P.; Rothuizen, H.; Schmid, H.; Schmidt-Winkel, P.; Stutz, R.; Wolf, H. *IBM J. Res. Dev.* **2001**, *45*, 697.] do not present the same problems because except for the step of stamp inking they are solvent-free. They are not compatible with the masking steps of conventional micro-nanofabrication techniques though.

(16) Miller, C.; Cuendet, P.; Grätzel, M. *J. Phys. Chem.* **1991**, *95*, 877.

(17) Liu, J.; Kaifer, A. E. *Isr. J. Chem.* **1997**, *37*, 235.

(18) Yan, D.; Saunders, J. A.; Jennings, G. K. *Langmuir* **2000**, *16*, 7562.

(19) Yan, D.; Jordan, J. L.; Burapatana, V.; Jennings, G. K. *Langmuir* **2003**, *19*, 3357.

(20) Dunbar, T. D.; Cygan, M. T.; Bumm, L. A.; McCarty, G. S.; Burgin, T. P.; Reinerth, W. A.; Jones, L.; Jackiw, J. J.; Tour, J. M.; Weiss, P. S.; Allara, D. L. *J. Phys. Chem. B* **2000**, *104*, 4880.

(21) Ishida, T.; Mizutani, W.; Tokumoto, H.; Choi, N.; Akiba, U.; Fujihira, M. *J. Vac. Sci. Technol., A* **2000**, *18*, 1437.

(22) Leatherman, G.; Durantini, E. N.; Gust, D.; Moore, T. A.; Moore, A. L.; Stone, S.; Zhou, Z.; Rez, P.; Liu, Y. Z.; Lindsay, S. M. *J. Phys. Chem. B* **1999**, *103*, 4006.

(23) Patrone, L.; Palacin, S.; Bourgoin, J. P.; Lagoute, J.; Zambelli, T.; Gauthier, S. *Chem. Phys.* **2002**, *281*, 325.

(24) Stuhr-Hansen, N.; Christensen, J. B.; Harrit, N.; Bjornholm, T. *J. Org. Chem.* **2002**, *68*, 1275.

(25) van Stam, J.; Imans, F.; Viaene, L.; De Schryver, F. C.; Evans, C. H. *J. Phys. Chem. B* **1999**, *103*, 5160.

(26) Puvvada, S.; Blankschtein, D. *J. Chem. Phys.* **1990**, *92*, 3710.

(27) (a) Brust, M.; Walker, M.; Bethell, D.; Schiffrin, D. J.; Whyman, R. *J. Chem. Soc., Chem. Commun.* **1994**, 801. (b) Bourgoin, J. P.; Kergueris, C.; Lefevre, E.; Palacin, S. *Thin Solid Films* **1998**, *327*, 515. (c) Brust, M.; Stuhr-Hansen, N.; Norgaard, K.; Christensen, J. B.; Nielsen, L. K.; Bjornholm, T. *Nano Lett.* **2001**, *1*, 189. (d) Werts, M. H. V.; Lambert, M.; Bourgoin, J. P.; Brust, M. *Nano Lett.* **2002**, *2*, 43.

energy (nonwetting for water), suitable for the transfer of LB films of gold nanoparticles.

SAMs Preparation. *(a) Flat Gold Substrates.* SAMs of DT made from aqueous micellar solution (DT-Mi) and from ethanolic solution (DT-Eth) were made by immersing freshly prepared gold surfaces in the respective solutions for about 2 days. Insertion of conjugated molecules (T3, Se3, OPV3) was performed by dipping preformed DT SAM samples into the aqueous micellar solution of the conjugated molecule for a time ranging from ~1 to a few hours. Each immersion of a substrate in a solution was followed by carefully rinsing with the solvent (water for DT-Mi and conjugated molecules in aqueous micellar solution, ethanol for DT-Eth) and drying under a filtered dry nitrogen flow.

(b) LB Films of Gold Nanoparticles. Ligand exchange was performed by immersing the slides carrying the LB films in micellar solutions of T3 for various times. Control experiments using only micellar solutions without T3 were also carried out. After exposure, the glass slides were carefully rinsed with pure 18 MΩ·cm water and ethanol and dried with a stream of nitrogen.

UV−Visible Spectrometry. UV−visible spectra were measured on a Perkin-Elmer Lambda 900 spectrophotometer. For the measurements on the LB film of gold nanoparticles, a separate baseline was recorded for each silanized glass slide before LB transfer, stored, and used for obtaining spectra free of artifacts related to the glass slides. Difference spectra were obtained by subtracting the absorption spectrum of the nanoparticle LB film before immersion from the spectra of the LB film after immersion.

STM. STM experiments on the SAMs were performed at ambient conditions with a custom-made microscope. Pt/Ir cut tips were used, and the bias voltage was applied to the sample with respect to the grounded tip. The images were recorded in constant current mode. The imaging conditions were chosen so that the dodecanethiolate lattice was resolved, that is, with a typical tunneling resistance $R_{th} \geq 100$ GΩ.

Results and Discussion

Comparison of Water-Born and Ethanol-Born DT SAMs. PM-IRRAS spectra (not shown) recorded from DT-Mi and DT-Eth SAMs proved quite similar to those reported by Jennings et al.[18] In particular they showed the same differences corresponding to a 4% increase in the average SAM density of DT-Mi as compared to DT-Eth. This increased average SAM density was shown in ref 18 to go with a higher blocking current in electrochemical test experiments. The DT SAM on gold consists of domains of close-packed molecules forming ordered lattices separated by less-ordered areas composed of defect lines and pits one-gold-atom-step deep.[28] Those pits are covered with DT molecules which have the same close-packed arrangement as in the topmost layer, while the defect lines are also covered with DT molecules but in a less dense arrangement. These lines and the borders of the pits are contributing to the amount of molecular gauche conformation that shows up in the IRRAS spectra in the form of an increased $\nu_a(CH_2)$ line at about 2920 cm^{-1}.

To check the differences between DT-Mi and DT-Eth SAMs onto gold, we performed a comparative STM study. Figures 2 and 3 show typical STM images of these SAMs. The general features of the two types of SAMs are obviously quite similar at both scales. We focus first on the small scale images of Figure 2. To the best of our resolution, we could not detect any difference of molecular arrangement or lattice spacing between DT-Mi and DT-Eth SAMs. We performed in particular a systematic fast Fourier transform (FFT) analysis of the images recorded on both types of samples. Two examples of FFT are shown in the insets of Figure 2. The results of this analysis show that the lattice parameters of DT-Mi (4.97 ± 0.07 Å) and DT-Eth (5.00 ± 0.05 Å) only differ by ~0.6% [note, the DT-Eth lattice was used to calibrate the STM on the basis of the known parameters of the $\sqrt{3} \times \sqrt{3}R30°$ lattice].[28] Consequently, the increased average chain density evidenced by IRRAS[18] does not originate in a difference in the local packing of the molecules.

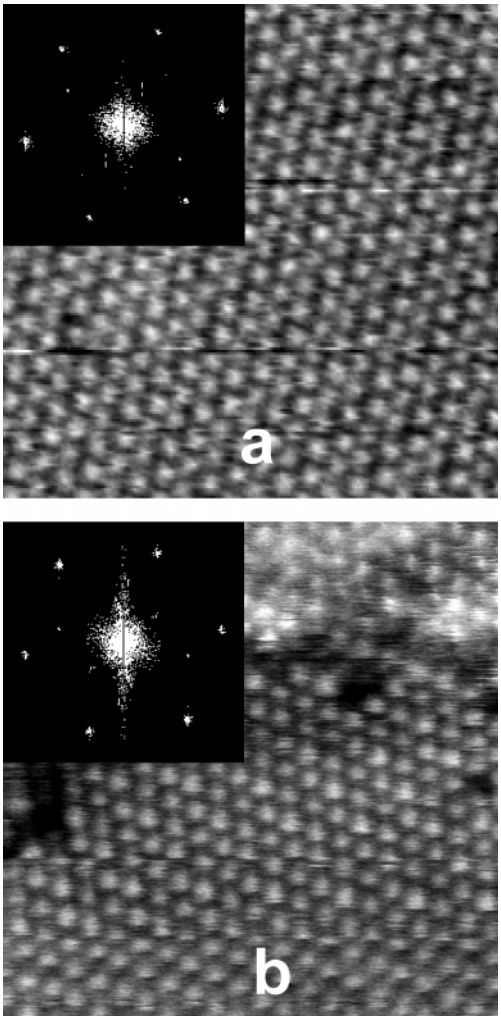

Figure 2. High-resolution STM images of DT SAMs on Au(111) formed from (a) ethanolic and (b) $C_{12}E_6$ aqueous micellar solutions. The images are 9 × 9 nm^2. Inset shows the typical two-dimensional Fourier transform of STM images.

Nevertheless, as illustrated in Figure 3, DT SAMs from aqueous micellar solution usually exhibit less etch pits and defectless boundaries between crystallized domains. Thus, the size of the domains is increased on average compared to the DT-Eth case. For instance, in Figure 3 one counts ~30 etch pits in DT-Mi SAM image instead of ~50 in the DT-Eth one. Domain boundaries also appear more pronounced in the latter. Jennings et al. concluded from their studies that the DT-Mi had an increased density of alkyl chains compared to the DT-Eth with an increase of the average chain tilt of 5°.[18] Our results clearly show that the increase in chain density is not due to a change in packing structure of the layer but rather results from a reduced defect density at domain boundaries and etch pits. This substantiates the conclusion reached by Jennings et al.[18] by a direct observation. Our conclusion is supported by a more recent work of the same authors[14] showing that the use of an aqueous solvent is more favorable to complete the SAM defects with alkylthiol molecules embedded in micelles. Such behavior may explain our observation of defectless larger domains in the case of water-born DT SAMs.

(28) Delamarche, E.; Michel, B.; Biebuyck, H. A.; Gerber, C. *Adv. Mater.* **1996**, *8*, 719.

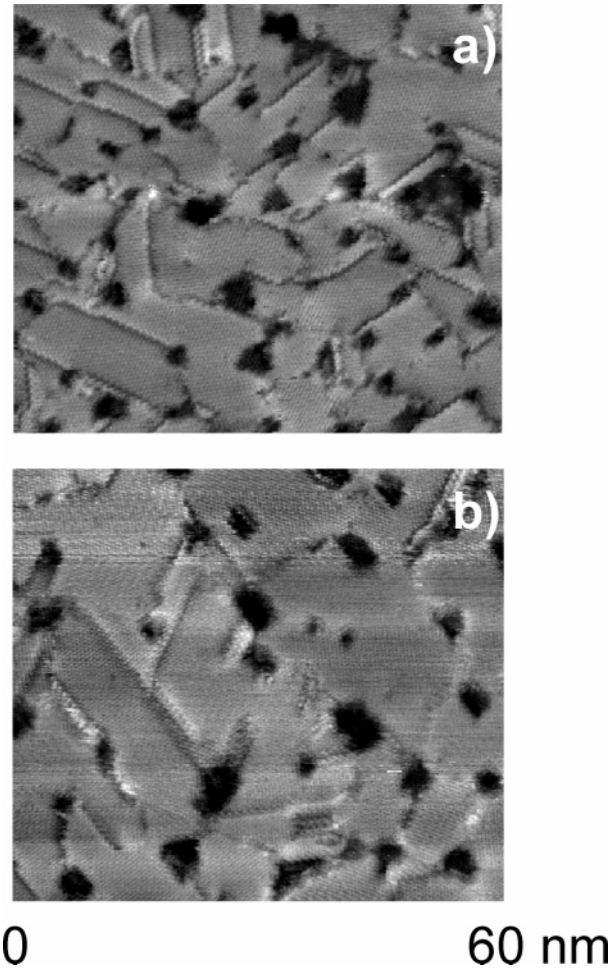

Figure 3. STM images of a typical DT SAM on Au(111) from (a) ethanol and (b) aqueous micellar solutions. Images size is 60×52 nm^2.

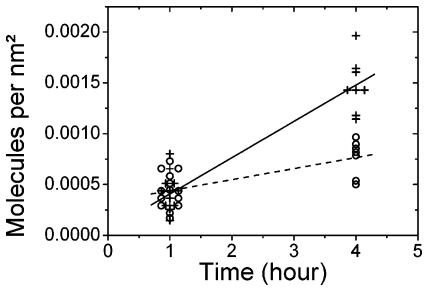

Figure 4. Comparison of the number of T3 molecules inserted in DT-Eth (+) and in DT-Mi (○) SAMs for two dipping times. Solid and dashed lines are linear fits for DT-Eth and DT-Mi, respectively.

To further probe the consequences of the improvement in SAMs quality when preparing them from micelles rather than from ethanolic solutions, we studied by STM the kinetics of insertion of thiol-terminated conjugated molecules into the two types of SAMs.[8,21,23] As a probe, we used the T3 molecule, the insertion of which is known to occur predominantly at defects,[23] that is, etch pits, step edges, and boundaries between crystallized domains of DT. The results are shown in Figure 4 for two dipping times (1 and 4 h) of the DT SAM in T3 solution prepared in 1,1,1-tricholoroethane. Although similar after 1 h of immersion, it clearly appears that the insertion is more efficient in DT-Eth than in DT-Mi after 4 h. This is consistent with a reduced number of etch pits and defects in the domain boundaries in DT SAMs self-assembled from aqueous micellar solution as compared to ethanol.

Conjugated Molecules in Aqueous Micellar Solution: Preparation and Insertion in the DT SAM on Au(111). Because self-assembling conjugated molecules is of particular interest in molecular electronics,[29] we then extended the aqueous micellar solution technique of SAM formation to various conjugated molecules. In this case, it was necessary to stir the solution under ultrasonic treatment during several hours, in agreement with the work of van Stam et al.[25] who prepared aqueous micellar solutions of α-terthiophene. Moreover in our experiments the solution was then centrifuged and filtered to extract the clear supernatant part. These solutions were checked by UV−visible experiments showing similar spectra as for T3 or Se3 in 1,1,1-trichloroethane and OPV3 in chloroform. Trying to make a solution of these conjugated molecules directly in water failed as proved by the absence of the UV−visible signal, thus, demonstrating that micelles are necessary for solvating such hydrophobic molecules even in minute amounts [note, the aqueous solubility of T3 is less than 10^{-7} M].[30] Direct adsorption of these molecules from the aqueous micellar solution onto gold was carried out successfully as probed by STM experiments (not shown).

As a second step, we studied the insertion of these conjugated molecules in alkanethiol SAMs on flat Au(111) surfaces from aqueous micellar solutions. The samples were prepared as reported in a previous paper.[23] After insertion, the samples were carefully rinsed with deionized water and dried under a nitrogen flux. STM experiments showing bright spots after inserting the conjugated molecules in a DT-Eth SAM are presented in Figure 5 for Se3 and OPV3. These images are similar to those obtained after direct insertion from organic solvents.[23] These spots are interpreted as conjugated molecules inserted in the DT layer. As in the case of organic solvents, the insertion was observed to proceed mainly at defect sites of DT (domain boundaries, etch pits) and very seldom in the middle of a crystallized DT domain.[23] These molecules appear brighter in the constant current image because they are more conducting than the surrounding DT layer. Importantly, no difference was observed between the mixed SAMs prepared from micellar solutions and the mixed SAMs prepared from organic solutions when comparing the apparent height of the conjugated molecule with respect to the DT.[23] However, we could notice that insertion of conjugated molecules from the aqueous micellar solution is much more efficient. For the same dipping times we estimated an increase of the number of inserted conjugated molecules by a ratio of 40−50 with micelles compared to chlorinated solutions. Such observations are consistent with the aforementioned recent study by Jennings and co-workers.[14] They found that a micellar aqueous solution is more efficient to deliver alkylthiol molecules at defect sites (from exposure times ≥ 1 h) as compared to ethanol. This last stage of SAM formation is indeed comparable to the insertion process of conjugated molecules filling the remaining defects in the preformed alkylthiol SAM.

Ligand Exchange of Conjugated Molecules from the Aqueous Micellar Solution with DT Grafted on the Surface of Film-Deposited Gold Nanoparticles. We then performed exchange of T3 molecules from the micellar aqueous solution with DT molecules on the

(29) Patrone, L.; Palacin, S.; Charlier, J.; Armand, F.; Bourgoin, J. P.; Tang, H.; Gauthier, S. *Phys. Rev. Lett.* **2003**, *91*, 096802.
(30) Downum, K. R.; Rodriguez, E. *J. Chem. Ecol.* **1986**, *12*, 823.

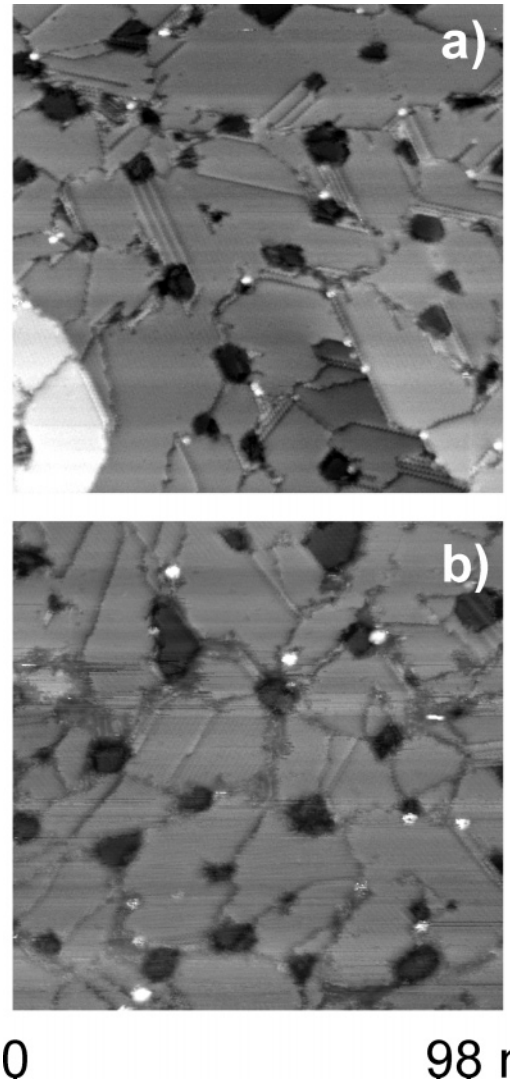

Figure 5. STM images of Se3 (a) and OPV3 (b) conjugated molecules inserted into the DT SAM on Au(111) from the aqueous micellar solution. The inserted conjugated molecules appear as bright spots. Note that the DT monolayers have been annealed, which explains their improved quality compared to those of Figure 3. Imaging conditions are $I_t = 1.9$ pA and $V_t = +0.78$ V.

surface of gold clusters. The ligand-exchange reaction of micelle-delivered T3 on LB films of DT-stabilized gold nanoparticles[27] was followed by UV−visible absorption spectrometry. Glass slides carrying a LB film of gold nanoparticles were immersed in aqueous micellar solutions of T3. After a given time of exposure, the slides were rinsed with deionized water and ethanol, and UV−visible absorption spectra were recorded (Figure 6). Upon exposure to a micellar T3 solution, a UV−visible absorption band at ~440 nm appears, corresponding to the $\pi-\pi^*$ electronic transition of T3. This band grows with exposure time and is identical to the band that appears when using an ethanolic T3 solution for the ligand exchange reaction.[31] The absorption maximum of T3 on the nanoparticle films has undergone a significant shift compared to that of T3 in solution (381 nm in 1,1,1-trichloroethane, 345 nm in water and micelles as shown in the Figure 6 inset). This points in the direction of the formation of T3−thiolate resulting from the strong interaction of the T3 with the particle surface through direct attachment of the T3 to

(31) Manuscript in preparation.

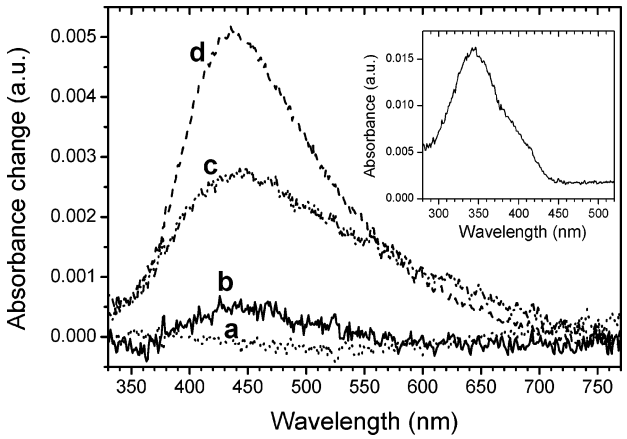

Figure 6. UV−visible difference spectra measured on LB films of DT-stabilized gold nanoparticles that have been immersed in the (a) bare aqueous micellar solution, (b) T3 aqueous micellar solution during 15 h, (c) T3 aqueous micellar solution during 4 days, and (d) T3 ethanolic solution (for comparison). Inset shows UV−visible spectrum measured on the T3 micellar aqueous solution.

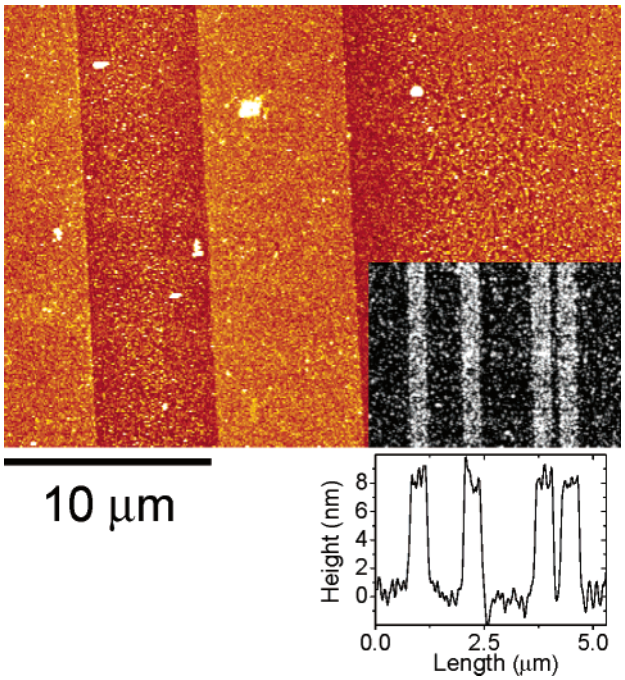

Figure 7. AFM tapping mode image of a patterned gold surface. The brighter areas correspond to stripes protected from etching by a SAM of DT prepared from the DT $C_{12}E_6$ aqueous solution. The stripes correspond to the places where the PMMA resist was irradiated by e-beam lithography, developed in MIBK/IPA and exposed to the DT $C_{12}E_6$ aqueous solution. The PMMA resist was then removed in trichloroethylene, and the sample was dipped into a ferricyanide-based etching solution. The inset is a close-up view of four 370-nm-wide lines. Stripe heights are ~8 nm as shown by the cross section.

the particles. These results indicate that T3 is inserted into the nanoparticle film and that it is bound to the particle surface: micelle delivery of T3 can, thus, be used to perform thiol exchange reactions on nanoparticle films.

From these experiments using DT-stabilized gold nanoparticles and DT SAMs, we, thus, conclude that aqueous micelles of $C_{12}E_6$ are good vectors for locally delivering conjugated molecules while keeping their reactivity.

DT-Mi SAM Deposition through a Lithographic Resist Mask. Besides its environmentally friendly prin-

ciple, another obvious advantage of using water-based solutions for preparing SAMs is that it renders SAMs formation compatible with standard lithography. To validate the principle of using SAMs in a standard process of microfabrication, we prepared a gold sample covered with a spun poly(methyl methacrylate) (PMMA) resist about 150-nm thick. Openings of various forms, the size of which ranged from 20 μm down to 200 nm in width, were then formed in the mask by e-beam irradiation followed by developing in methyl isobutyl ketone/2-propanol (1:3 MIBK/IPA). The sample was then exposed to UV−ozone for a few minutes to ensure cleaning of the gold surface at the bottom of the openings. We then adsorbed DT in the openings from a $C_{12}E_6$ aqueous micellar solution and performed afterward a lift-off in trichloroethylene to remove the resist. This process resulted in a protective SAM being formed at the place where the openings in the resist had been made. Indeed, dipping the sample in a ferricyanide-based solution of gold etchant [$K_3Fe(CN)_6$ solution][32] for 6 min positively revealed the pattern protected by the SAM as shown in Figure 7.

Conclusions

In this paper, we investigated SAMs prepared from aqueous micellar solutions. From STM and specific insertion experiments, we showed that the DT SAMs prepared from $C_{12}E_6$ solutions have increased domain size and less defects than their analogues prepared from ethanolic solutions. We showed that the local packing of the DT molecules is identical whether the SAMs were formed from ethanolic or from aqueous micellar solutions.

We also successfully used the same type of micelles as vectors for delivering thiol-terminated conjugated molecules that could be used to form SAMs onto gold surfaces, including gold nanoparticles, or be inserted in SAMs of DT. Finally, we proved that using aqueous micellar solutions allows to include SAMs in standard lithography techniques. We believe that these results are important because they considerably widen the possibilities of using SAMs in technological fabrication processes.

Acknowledgment. This work was funded by the European Community within the "Nanomol", Project No. IST-1999-12603. Dr. B. Michel and IBM Zürich are thanked for their kind donation of a scanning tunneling microscope that was used in this work. We also thank Thomas Bjornholm and Nicolai Stuhr-Hansen for providing us with OPV3 molecules.

LA048133B

(32) Xia, Y.; Zhao, X.-M.; Kim, E.; Whitesides, G. M. *Chem. Mater.* **1995**, *7*, 2332.